ENVIRONMENTAL RESEARCH
LETTERS

PURPOSE-LED PUBLISHING™ Part of the ENVIRONMENTAL RESEARCH SERIES

LETTER • OPEN ACCESS

Global multi-model trends of unsustainable irrigation under climate change scenarios

To cite this article: Andrea Citrini *et al* 2025 *Environ. Res. Lett.* **20** 104011

IOP Publishing Environ. Res. Lett. 20 (2025) 104011 https://doi.org/10.1088/1748-9326/adfcee

ENVIRONMENTAL RESEARCH
LETTERS

OPEN ACCESS

RECEIVED
5 May 2025

REVISED
12 August 2025

ACCEPTED FOR PUBLICATION
19 August 2025

PUBLISHED
2 September 2025

LETTER

Global multi-model trends of unsustainable irrigation under climate change scenarios

Andrea Citrini[1], **Matteo Sangiorgio**[2] and **Lorenzo Rosa**[1,*]

[1] Biosphere Sciences & Engineering, Carnegie Institution for Science, Stanford, CA 94305, United States of America
[2] Department of Electronics, Information and Bioengineering, Politecnico di Milano, Via Ponzio 34/5, 20133 Milan, Italy
* Author to whom any correspondence should be addressed.

E-mail: lrosa@carnegiescience.edu

Keywords: hydrology, irrigation, water sustainability, climate change, water scarcity, agriculture

Supplementary material for this article is available online

Abstract

Recent advances in hydrological modeling have quantified unsustainable irrigation water consumption (UIWC), underscoring its impacts on freshwater stocks depletion and environmental flows impairment. However, the long-term sustainability of irrigation under different climate change scenarios remains insufficiently explored. Here, we assess future trajectories of UIWC using an ensemble of simulations under a sustainable development pathway (SSP1-2.6) and a high-emissions pathway (SSP5-8.5), projecting changes through each decade until 2100. The baseline estimate of global UIWC is 458 km^3 yr^{-1}. Global UIWC is projected to increase under climate change, but multi-model projections show substantial uncertainty. By 2100, estimates range from 458 to 546 km^3 yr^{-1} under the low-emission SSP1-2.6 scenario, and from 456 to 638 km^3 yr^{-1} under the high-emission SSP5-8.5 scenario, highlighting divergent future outcomes depending on emissions pathways and model assumptions. Under baseline conditions, the Ganges, Sabarmati, and Indus basins have the highest UIWC. Climate change scenarios show divergent regional trends, with the SSP5-8.5 scenario projecting larger increases in UIWC—especially in the Ganges, Indus, and US High Plains—compared to SSP1-2.6. These increases reflect both greater climate impacts and higher model uncertainty. Normalizing UIWC by irrigated area reveals hotspots of irrigation pressure, particularly in South Asia and the Nile Delta, where per-area UIWC exceeds 50 mm yr^{-1}, and is projected to rise further under both scenarios. By assessing multi-model water scarcity risks in irrigated croplands, these findings provide crucial insights for guiding climate change adaptation strategies in agriculture.

1. Introduction

Irrigated agriculture is vital for global food production and a key strategy for adapting agriculture to climate change [1]. By providing a controlled water supply, irrigation helps mitigate the adverse effects of water scarcity, extreme heat, and unpredictable rainfall on crop yields [2]. Irrigation is responsible for approximately 90% of anthropogenic freshwater consumption and is implemented on 22% of cultivated land, enhancing yields compared to rainfed agriculture [3, 4]. This makes irrigation essential for ensuring food security [5, 6].

The availability and timing of freshwater are important factors limiting the expansion of food production through irrigation [7–9]. Globally, almost half of the water used for irrigation is unsustainable, exceeding local renewable water supplies [10]. Unsustainable irrigation depletes environmental flows and overuses freshwater resources, leading to groundwater over-extraction and river depletion [11–14]. Furthermore, an estimated 15% of unsustainable irrigation volumes are driven by international demand for agricultural products, exacerbating the depletion of water resources [10, 15, 16]. Declining water quality due to rising and emerging

pollutants—such as excess nitrogen from agriculture and urban runoff—worsens water scarcity by making water unsafe for ecosystems and human use, further limiting its availability [17–19]. This poses a serious threat to both local and global water and food security [20, 21].

Climate change presents major challenges to the sustainability of irrigation practices by disrupting precipitation patterns, increasing the frequency of extreme weather events, and intensifying droughts and floods [22–24]. These climate-induced changes reduce the availability of freshwater resources while simultaneously raising crop water demands, making irrigation water management more challenging [24, 25]. Therefore, managing water for agriculture in a warming climate requires more efficient and adaptive strategies to ensure long-term resilience and sustainability [26].

Assessing the water sustainability of irrigation in the world's major irrigation regions under 21st century warming scenarios is essential for understanding future agricultural resilience [27, 28]. Previous research has examined water demand in relation to local renewable water supplies, exploring various quantitative aspects of water scarcity in irrigated agriculture under both historical and future climate conditions [29–35]. Despite these contributions focusing on the impacts of climate change on irrigation, multi-model and multi-decadal analyses to evaluate both historical and future water scarcity in irrigated agriculture providing explicit time trajectories of decadal volumes through the end of the 21st century is overlooked.

Here, we quantify monthly unsustainable irrigation water consumption (UIWC) at a 30-arcminute resolution (∼50 km at the Equator) under two climate change scenarios for the 21st century. The use of a temporally explicit framework allows for more precise prioritization of adaptation strategies, providing essential insight into how global warming will impact the long-term viability of irrigation. We assess monthly UIWC volumes by evaluating the extent to which water consumption surpasses locally renewable water availability, leading to the depletion of groundwater, rivers, and environmental flows [21]. We assess UIWC based on the 2015 global irrigation extent [36], the most up-to-date and comprehensive dataset of irrigated areas worldwide. To account for a range of possible outcomes, we draw on outputs from five distinct climate models and two hydrological models from the Coupled Model Intercomparison Project (CMIP6) archive [37]. This allows us to analyze unsustainable irrigation under baseline conditions as well as two future climate scenarios: SSP1-2.6 (sustainable development) and SSP5-8.5 (high emissions) [22]. In total, we evaluated 20 future scenarios derived from 10 combinations of climate and hydrological models under the two climate change scenarios, namely SSP1-2.6 and SSP5-8.5. First, we employ geospatial clustering techniques to identify and delineate 329 irrigation regions (IRs) worldwide. An IR is defined as a specific geographical area where water resources are managed and allocated for irrigation. Second, using a process-based water balance model that includes environmental flow requirements [10, 21, 38–41], we estimate monthly renewable water availability from CMIP6 surface and sub-surface runoff projections. Third, we acknowledge the variability inherent in the 20 combinations of climate and hydrological models and emphasize the importance of accounting for this uncertainty in our projections. Therefore, we assess renewable water availability against irrigation water consumption for each future climate scenario and climate model, quantifying UIWC at a global pixel-level scale. Fourth, we present the results at the IR scale, showcasing variations in UIWC across the 20 future scenarios analyzed in this study. For each IR and future scenario, we quantify the volumes of UIWC, the level of reliance on it, and the emerging trends.

By leveraging ensemble projections from both climate and hydrological models, and by incorporating environmental flow requirements directly into a water balance, our approach enables a more uncertainty-aware evaluation of future water sustainability risks, highlighting the heterogeneous nature of climate impacts on irrigation sustainability not only spatially but also through the decades. This comprehensive multi-model quantification of irrigation water sustainability provides a robust basis for comparing regions worldwide, evaluating emerging risks and the exacerbation of water scarcity among them, offering essential information for policy-making and effective adaptation to water scarcity.

2. Methods

We mapped global IRs and used climate outputs from five climate models and two hydrological models in the CMIP6 archive to quantify unsustainable irrigation water consumption for the baseline period of 2001–2010 and for each decade through 2100 under two climate change scenarios: a sustainable development pathway (SSP1-2.6) and a high-emissions pathway (SSP5-8.5). SSP1-2.6 envisions a future focused on sustainable practices, aiming for net-zero emissions by 2050, limiting global temperature rise to approximately 1.8 °C by the end of the century, and with substantial improvements in irrigation efficiency and sustainable water management [22]. In contrast, SSP5-8.5 reflects a *business-as-usual* scenario, heavily reliant on fossil fuels, with projected global warming up to 4.4 °C by 2100 and increases in water consumption due to the expansion of irrigated areas to meet growing food demand [22]. These scenarios represent distinct socioeconomic trajectories and greenhouse gas emissions pathways, providing insights into potential climate outcomes

based on varying human behavior and policy choices [22, 42].

We define UIWC as the volume of water consumed for irrigation that exceeds the renewable supply from rivers, lakes, and shallow aquifers replenished by precipitation [10, 21]. For each scenario, UIWC is quantified by solving a water balance model at a 30-arcminute resolution (∼50 km at the Equator), using monthly surface and subsurface runoff data, along with water consumption data derived from CMIP6 climate model outputs [37].

2.1. Mapping of irrigation regions

We map 329 IRs worldwide. We define an IR as a specific geographic area where water resources are managed and distributed for agricultural irrigation. Each IR encompasses both the areas where water is distributed to agricultural fields via canals, pumps, and pipes, and the upstream highland areas that hydrologically contribute to the region's water supply. We mapped IRs by filtering out grid cells in which the area equipped for irrigation was <5% of the total grid-cell area (5-arcminute), based on the 2015 Global Area Equipped for Irrigation dataset (G_AEI) [36]. Cells below this threshold were deemed to have negligible influence on total irrigation water consumption. Then, we established pixel clusters using the *Region Group spatial analyst* tool in a GIS environment. This approach allows performing a zone grouping based on the geometric connectivity among the pixels containing values. We utilized the '*Eight ways*' mode, which considers connectivity between pixels both orthogonally and diagonally, considering diagonal neighbors (northwest, northeast, southwest, southeast), thus capturing more intricate, contiguous clusters. These clusters were further reviewed, associated, and, if necessary, separated according to hydrological criteria by intersecting them with Level 6 hydrological basins from the HydroBASIN database [43]. The analysis of IRs was conducted starting from the spatial resolution of the G_AEI dataset (5 arcminutes, ∼10 km at the equator) and resulted in polygonal units suitable for aggregating and presenting UIWC estimates at the sub-regional scale. While IR shares similarities with 'irrigation district' [44], IR focuses on the physical territory where irrigation practices take place without implying any formal administrative or legal oversight.

2.2. Blue water flows and water consumption data

Following previous work [10, 16, 20, 21, 38, 40, 41, 45, 46], we assessed renewable water availability using as input the blue water flows under baseline and future climate scenarios. This variable includes both surface water and seasonally renewable groundwater, without parsing them separately. The estimated monthly local surface and groundwater inflow for the baseline climate was derived from reference model runs from PCR-GLOBWB 2.0 [47], which was semi-calibrated using data from the Global Runoff Data Centre. For future climate scenarios, we utilized CMIP6 data under two climate change scenarios (SSP1-2.6 and SSP5-8.5) and retrieved monthly input data from two hydrological models H08 [48, 49] and WaterGAP2-2e [50] forced with outputs from five global climate models (GFDL-ESM4, UKESM1-0-LL, MPI-ESM1-2-HR, IPSL-CM6A-LR, and MRI-ESM2-0), with socioeconomic conditions fixed to the year 2015, provided by ISIMIP 3b [51]. In total, we analyzed 20 climate outputs: 10 for the sustainable development pathway (SSP1-2.6) and 10 for the high-emissions pathway (SSP5-8.5).

We calculated the difference between projected and baseline blue water input for each climate output and then applied this difference to the baseline reference input data. This approach, commonly used in climate model analysis [39, 40, 52], involves adding the perturbation (i.e. the model-specific projected climate minus the model-specific historical climate) to reference climate data. This adjustment accounts for discrepancies in historical climate simulations across models, the limitations in baseline data, and varying assumptions about climate-forcing factors like aerosols and cloud cover, which significantly affect regional precipitation patterns and land use [53].

Water consumption is calculated as the total water use for irrigation, livestock, electricity generation, domestic, mining, and manufacturing. Baseline monthly water consumption for these sectors is sourced from Huang *et al* [54], which provides data from four hydrological models (WaterGAP, H08, LPJmL, PCR-GLOBWB) for the period 2001–2010. Future monthly irrigation water consumption data do not account for the CO_2 fertilization effect. Although elevated CO_2 generally increases photosynthetic water-use efficiency [55], the net effect on crop evapotranspiration and irrigation demand remains uncertain and varies with crop type, soil properties, nutrient availability, and climate conditions [2]. Projections are derived from CMIP6 outputs under two climate change scenarios (SSP1-2.6 and SSP5-8.5), using five global climate models (GFDL-ESM4, UKESM1-0-LL, MPI-ESM1-2-HR, IPSL-CM6A-LR, and MRI-ESM2-0) and two global hydrological models (H08 and WaterGAP2-2e). As for blue water flows, to estimate future irrigation water consumption, we added the projected difference between historical and future values to the baseline consumption. Since irrigated agriculture accounts for 90% of global water consumption, water consumption for other sectors—livestock, electricity generation, domestic, mining, and manufacturing—was assumed to remain constant across the different climate change scenarios [38, 40, 41, 56].

2.3. Assessment of renewable water availability

Renewable blue water availability at a 30 arc-minute resolution was assessed by calculating the difference

between the blue water flows generated within each grid cell and the environmental flow requirements [46]. This availability includes both surface water and groundwater volumes replenished through the hydrological cycle. Monthly blue water flows were determined using local runoff estimates, which were calculated via an upstream–downstream flow accumulation routing module [10, 20, 21, 39, 40]. Blue water flows enter a grid cell either as local runoff (both surface and subsurface) or as inflows from upstream grid cells along river networks. To protect the health of aquatic ecosystems, a portion of blue water flows must be reserved for environmental needs [12]. Environmental flow requirements were estimated using the Variable Monthly Flow method [57], which accounts for the seasonal variations in blue water flows.

2.4. Assessment of unsustainable irrigation water consumption and reliance on unsustainable practices

We identified areas of UIWC as pixels where local water consumption exceeds renewable blue water resources [10, 21]. For each climate scenario, climate model, month, and pixel, unsustainable irrigation occurs when water consumption surpasses available water. The volume of UIWC is calculated as the difference between water consumption and renewable water availability in each pixel. UIWC is aggregated at the IR scale by summing the monthly values across all pixels within the region. By aggregating our pixel-level results at the IR scale, we ensure that our water sustainability assessments accurately reflect any potential water management interventions at the catchment level. The percentage of dependence on unsustainable practices was calculated by dividing UIWC volumes by the total water consumption for each IR.

3. Results

3.1. Volumes and emerging trends

We quantify monthly UIWC for each of the 20 multi-model scenarios at ∼50 km resolution pixel level worldwide, then aggregate the pixel-level UIWC data to the scale of individual IRs (supplementary figures 1 and 2). Figure 1 illustrates global trends in UIWC, as well as the top 20 IRs by water consumption. The shaded area represents the interquartile range, capturing the variability across multiple models. Under baseline conditions, global UIWC is 458 km^3 yr^{-1} (figure 1(a)). However, climate change scenarios reveal divergent futures for UIWC. By 2100, under the SSP1-2.6 scenario, global UIWC is projected to rise moderately to 494 km^3 yr^{-1}, an increase of 36 km^3 yr^{-1} compared to baseline, with potential variability among scenarios ranging from 458 km^3 yr^{-1} to 546 km^3 yr^{-1} (figure 1(a)). In contrast, the high-emission SSP5-8.5 scenario projects a more considerable increase, with UIWC reaching 571 km^3 yr^{-1} (+113.3 km^3 yr^{-1}) and a wider uncertainty range among scenarios spanning from 456 km^3 yr^{-1} to 638 km^3 yr^{-1} (figure 1(a)).

Under baseline climate conditions, the Ganges River basin has the highest UIWC at 54.8 km^3 yr^{-1}, followed by the Sabarmati (54.7 km^3 yr^{-1}), Indus (26.8 km^3 yr^{-1}), Tigris-Euphrates Lower Basin (21.2 km^3 yr^{-1}), and Nile Delta (18.2 km^3 yr^{-1}) (figure 1; figure 2(a)). However, the two climate change scenarios, SSP1-2.6 and SSP5-8.5, reveal contrasting trends in UIWC, with SSP5-8.5 showing greater variability and increase over time (figure 1).

Under SSP1-2.6, the Ganges River is projected to see the largest increase in UIWC, with additional UIWC volumes of +12.1 km^3 yr^{-1} by 2050, and +15.5 km^3 yr^{-1} by 2100 (figure 1(b); figures 2(b) and (c)). The Indus River follows, rising UIWC by +8.6 km^3 yr^{-1} by 2050, and +6.7 km^3 yr^{-1} by 2100 (figures 2(b), (c) and 3(a)). The US High Plains also shows a moderate rise, with increases of UIWC by +2.4 km^3 yr^{-1} by 2050, and +2.5 km^3 yr^{-1} by 2100 (figures 2(b), (c) and 3(a)).

In contrast, under SSP5-8.5, the Ganges River is projected to experience even more substantial UIWC increases, reaching +12.8 km^3 yr^{-1} (2050), and +18.0 km^3 yr^{-1} (2100) (figures 2(d), (e) and 3(a)). Similarly, the Indus River sees larger gains, with UIWC rising by +11.6 km^3 yr^{-1} (2050), and +15.3 km^3 yr^{-1} (2100) (figures 2(d), (e) and 3(a)). The US High Plains also shows sharper increases in UIWC under SSP5-8.5, with +3.6 km^3 yr^{-1} (2050), and +7.5 km^3 yr^{-1} (2100) (figure 1(c), 2(d), (e) and figure 3(a)). These differences highlight the higher impacts of climate change on UIWC under the high-emission scenario. Several IRs, such as the Ganges, Sabarmati, and California Central Valley, display statistically significant positive trends in projected UIWC, particularly under SSP5-8.5, whereas other areas (including the Ziya River and Nile Delta) exhibit non-significant or even negative trends (see supplementary table 1). While significance testing helps assess the robustness of these trends, the presence of a positive or negative slope itself can still indicate emerging directional changes that merit attention. Evaluating both the magnitude and significance of such trends is essential for understanding the spatial heterogeneity of irrigation challenges under future climate scenarios.

Climate Change projections also show decreases in UIWC and different trends between the two scenarios. For example, the Sabarmati River shows marked increases in UIWC under the SSP5-8.5 scenario, rising from 54.7 km^3 yr^{-1} by +1.6 km^3 yr^{-1} in 2050, and +5.9 km^3 yr^{-1} in 2100 (figures 1(b) and 2). This contrasts with the SSP1-2.6 scenario, where the projected behavior remains generally stable but

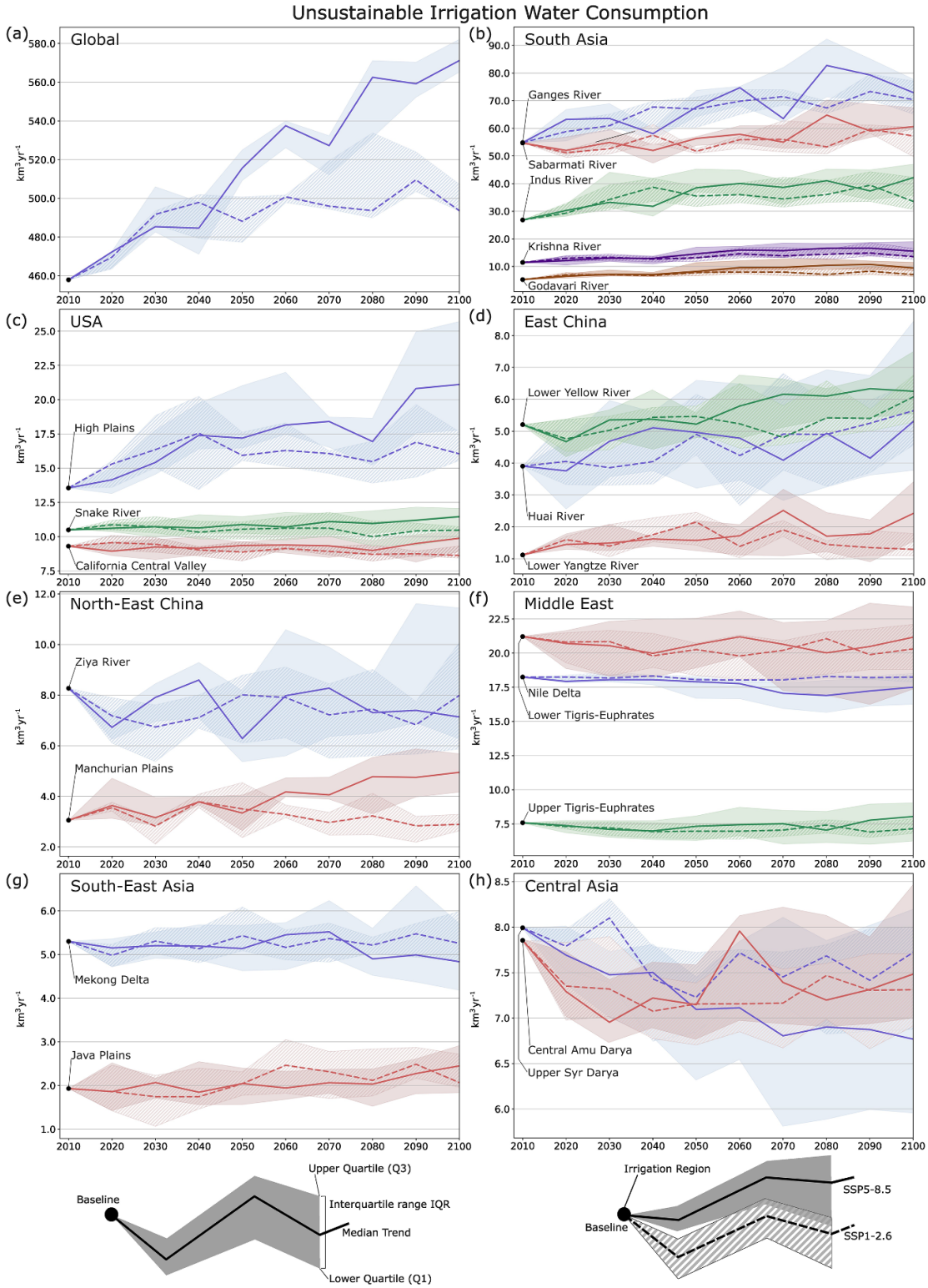

Figure 1. Multi-model trends of UIWC under SSP1-2.6 and SSP5-8.5 scenarios. The projected future trends of UIWC are based on the multi-model ensemble of 10 combinations between two hydrological models (H08 and WaterGAP2-2e) and five climate models (IPSL-CM6A-LR, UKESM1-0-LL, GFDL ESM4, MPI-ESM1.2-HR, and MRI-ESM2.0). The figure shows UIWC trends (a) worldwide and for (b)–(h) 20 irrigation regions with the highest water consumption (supplementary figure 2). The multi-model variability of the results is represented by the shaded area, which indicates the interquartile range; lines show the multi-model median value. Linear trends and their statistical significance for each median trajectory are reported in supplementary table 1.

with occasional UIWC decreases, such as a decrease of -3.0 km^3 yr^{-1} in 2050 (figures 1(b) and 2(b)). Decreases in UIWC around 1 km^3 yr^{-1} at the end of the century are expected for Lower Tigris-Euphrates -0.9 km^3 yr^{-1} under SSP1-2.6 (figures 1(f) and 2(c)), for the Upper Syr Darya (-1.2 km^3 yr^{-1}), Ziya river (-1.1 km^3 yr^{-1}), and Nile Delta (-0.7 km^3 yr^{-1}) under the high emission scenario (figure 2(e)).

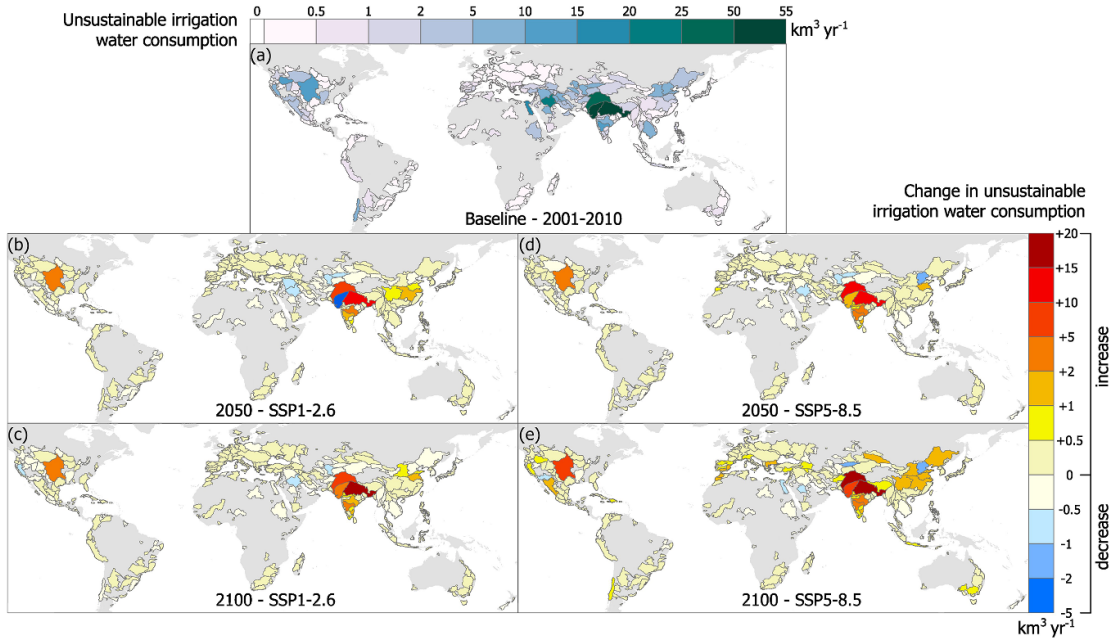

Figure 2. Multi-model median ensemble volumes of UIWC under SSP1-2.6 and SSP5-8.5 scenarios in 2050 and 2100. (a) UIWC in the baseline period (km^3 yr^{-1}). Change in UIWC (km^3 yr^{-1}) under SSP1-2.6 in 2050 (b) and 2100 (c), and under SSP1-8.5 in 2050 (d) and 2100 (e). Supplementary figures 3 and 4 show UIWC considering upper and lower quartile among the 20 future scenarios considered in this study.

Normalizing UIWC by IR areas enables a more spatially resolved assessment of regional irrigation pressure that is otherwise masked when aggregating volumes at the basin scale (figure 3(b)). Several IRs (e.g. Sabarmati River, Nile Delta, and Ganges River) exhibit markedly high values of UIWC per unit area under baseline conditions, exceeding 50 mm yr^{-1} in some cases (figure 3(b)). These values indicate intensive UIWC concentrated over relatively confined irrigated areas. Projections under SSP1-2.6 indicate increased UIWC across most of the top 20 IRs by water consumption by the end of the century. Several IRs across the Indian Peninsula (such as the Ganges, Sabarmati, Indus, Krishna, and Godavari Rivers) emerge as among the most affected in terms of UIWC increases, with average increments ranging from +8 to +15 mm yr^{-1} by 2100 under the SSP1-2.6 and SSP5-8.5 scenarios, respectively (figure 3(b)).

3.2. Most affected IRs

Figure 4 presents projections of changes in UIWC from the baseline climate for two sets of IRs: the 20 with the highest irrigation demand and the 20 most impacted IRs, projected through 2100 for both SSP1-2.6 and SSP5-8.5 climate scenarios. The most impacted IRs were selected based on the most considerable UIWC differences between baseline and 2100, excluding the top 20 by consumption, ensuring diverse regions are represented.

Among the IRs with the highest irrigation consumption, substantial changes in UIWC are observed, especially from mid-century onwards, with Asian and American regions experiencing large increases under the SSP5-8.5 scenario (figure 4(a)). The Ganges River shows the most drastic changes, with UIWC increasing by 28% under SSP1-2.6 and 33% under SSP5-8.5 by 2100 (figure 4(a)). Similar increases in UIWC are observed in other regions like the Indus River, Krishna River, US High Plains, Java Plains, Huai River, and Lower Yellow River, though starting from lower UIWC volumes than the Ganges (figure 4(a)). The Lower Yangtze and Godavari Rivers exhibit the largest increases in UIWC, reaching 117% and 80%, respectively, by 2100 under SSP5-8.5 (figure 4(a)).

The 20 most impacted IRs show how regions, particularly in South Asia and the Mediterranean, will see drastic UIWC increases, with some regions doubling UIWC with respect to the baseline, signaling extreme water vulnerability (figure 4(b)). Under SSP5-8.5, many regions will experience severe water scarcity by mid-century, with some already stressed by the first decades of the century. Hispaniola Island is projected to see fivefold increases in UIWC, while the Po Plain (Italy), Tavoliere Plain (Italy), and Garonne River (France) will fourfold their 2001–2010 UIWC levels (figure 4(b)).

3.3. Reliance on unsustainable irrigation practices

We present UIWC as a function of total water consumption for each IR (figure 5, supplementary figure 5), quantifying the share of irrigation water that exceeds locally renewable resources and offering insights into the sustainability of water use in specific regions. By expressing UIWC to total

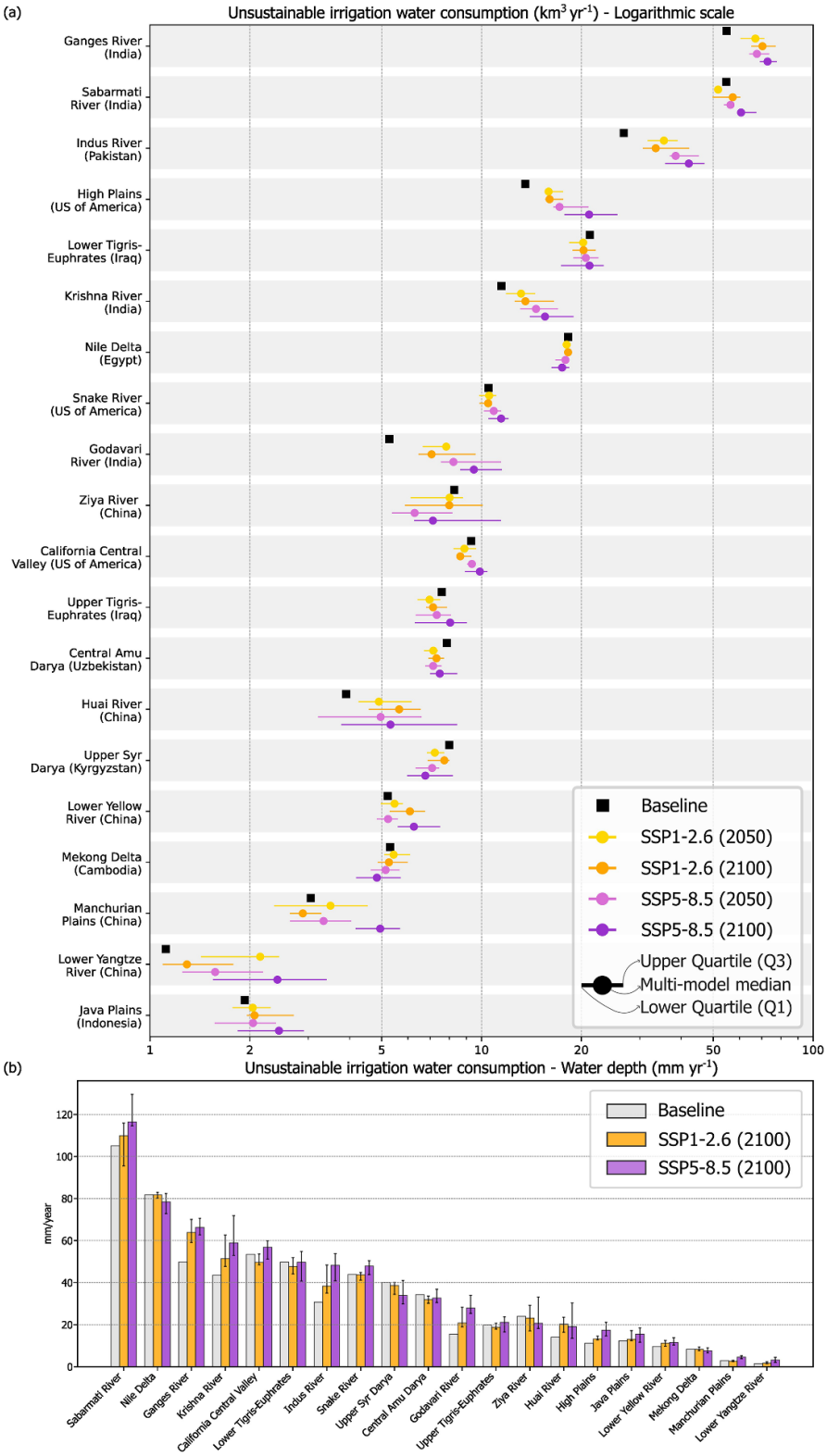

Figure 3. Projected changes in UIWC across the top 20 irrigation regions by water consumption. (a) Multi-model median and interquartile ranges of UIWC ($km^3\ yr^{-1}$, logarithmic scale) for baseline and future scenarios under SSP1-2.6 and SSP5-8.5 for 2050 and 2100. (b) UIWC expressed as water depth ($mm\ yr^{-1}$) for the top 20 irrigation regions ranked by annual irrigation water consumption. Interval bars show the range of UIWC due to the multi-model ensemble of 10 combinations between two hydrological models (H08 and WaterGAP2-2e) and five climate models (IPSL-CM6A-LR, UKESM1-0-LL, GFDL ESM4, MPI-ESM1.2-HR, and MRI-ESM2.0).

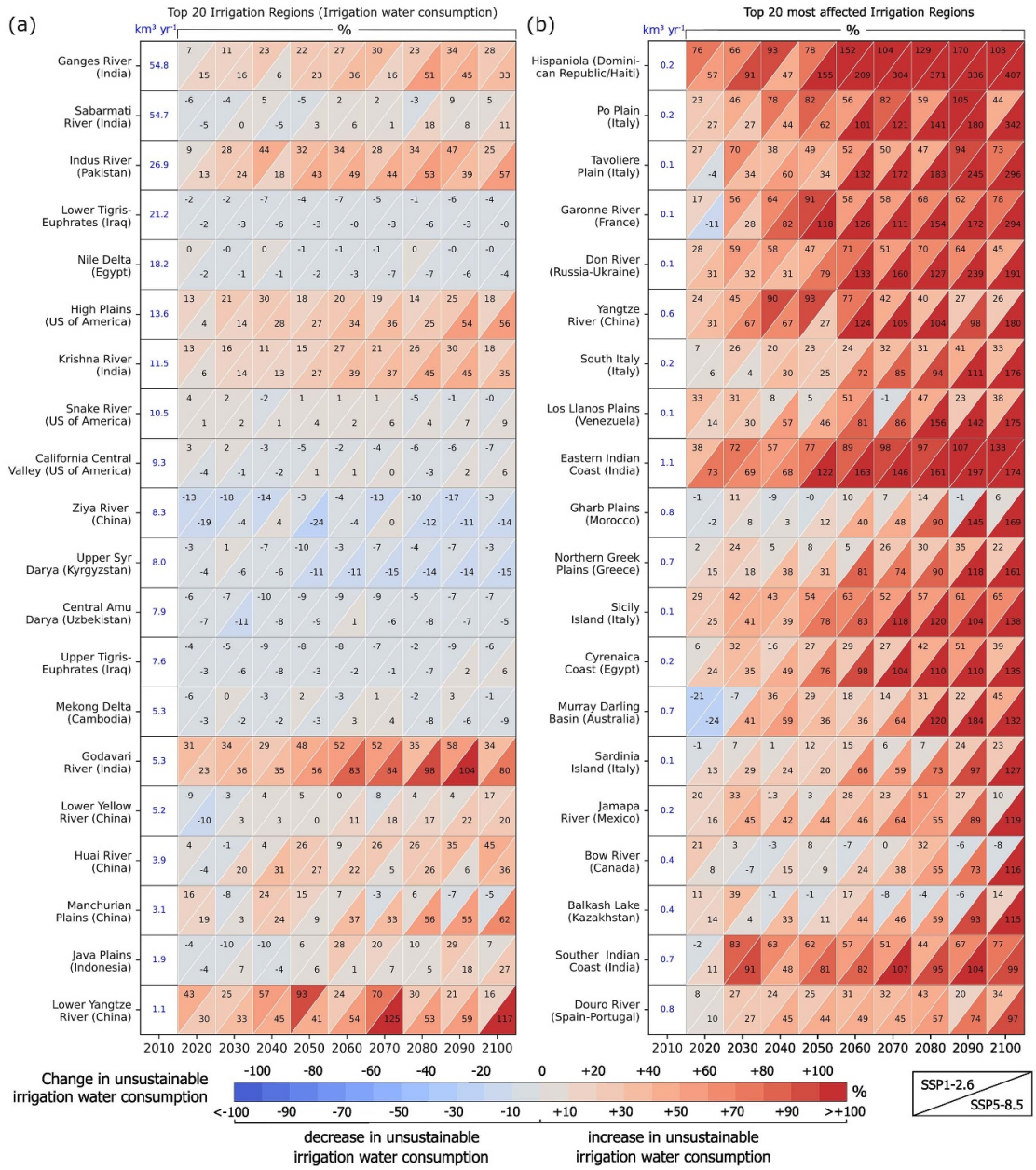

Figure 4. Decadal change in UIWC for the top 20 irrigation regions by water consumption and the top 20 most affected regions globally till 2100. The projections are shown as a percentage change in UIWC relative to the baseline year 2010. The portrait diagrams show the top 20 by irrigation demand (a) and the top 20 affected (b) irrigation region trends in terms of multi-model median percentage change of UIWC over baseline. The 20 affected irrigation regions were selected from those experiencing the most considerable UIWC volume differences between baseline and 2100 for SSP1-2.6 and SSP5-8.5 scenarios (excluding the top 20 with the highest irrigation water demand). The first column of the portrait diagrams represents the baseline values of UIWC in $km^3\ yr^{-1}$. Each other cell is split diagonally, representing two distinct climate scenarios: SSP1-2.6 (top left) and SSP5-8.5 (bottom right). The color gradient indicates percentage deviations from the baseline, ranging from +100% (red) to −100% (blue).

consumption, we highlight the extent to which each IR relies on unsustainable practices, providing a clearer understanding of regional vulnerabilities and informing targeted interventions for improving water sustainability. Higher ratios indicate that a pronounced portion of irrigation demand is unsustainable.

Under baseline climate conditions, IRs with the highest UIWC ratios, exceeding 90%, are predominantly in the MENA region (e.g. Tabuk Plains, Great Man-Made River, Al-Jouf Plains, Wadi al-Dawasir, Al-Kharj Plains, and Al-Qassim Plains) and western Mexico (Santo Domingo Valley) (figure 5, supplementary figure 5(a)). Among the top 20 regions for irrigation consumption, IR that exhibit an extensive reliance on unsustainable practices are the Sabarmati River (80%), Snake River (66%), Central Amu Darya (65%), Lower Tigris-Euphrates (61%), Upper Syr Darya (57%), the Central Valley of California (55%), the US High Plains (52%), the Nile Delta (51%), and the Ganges River (49%) (figure 5, supplementary figure 5(a)).

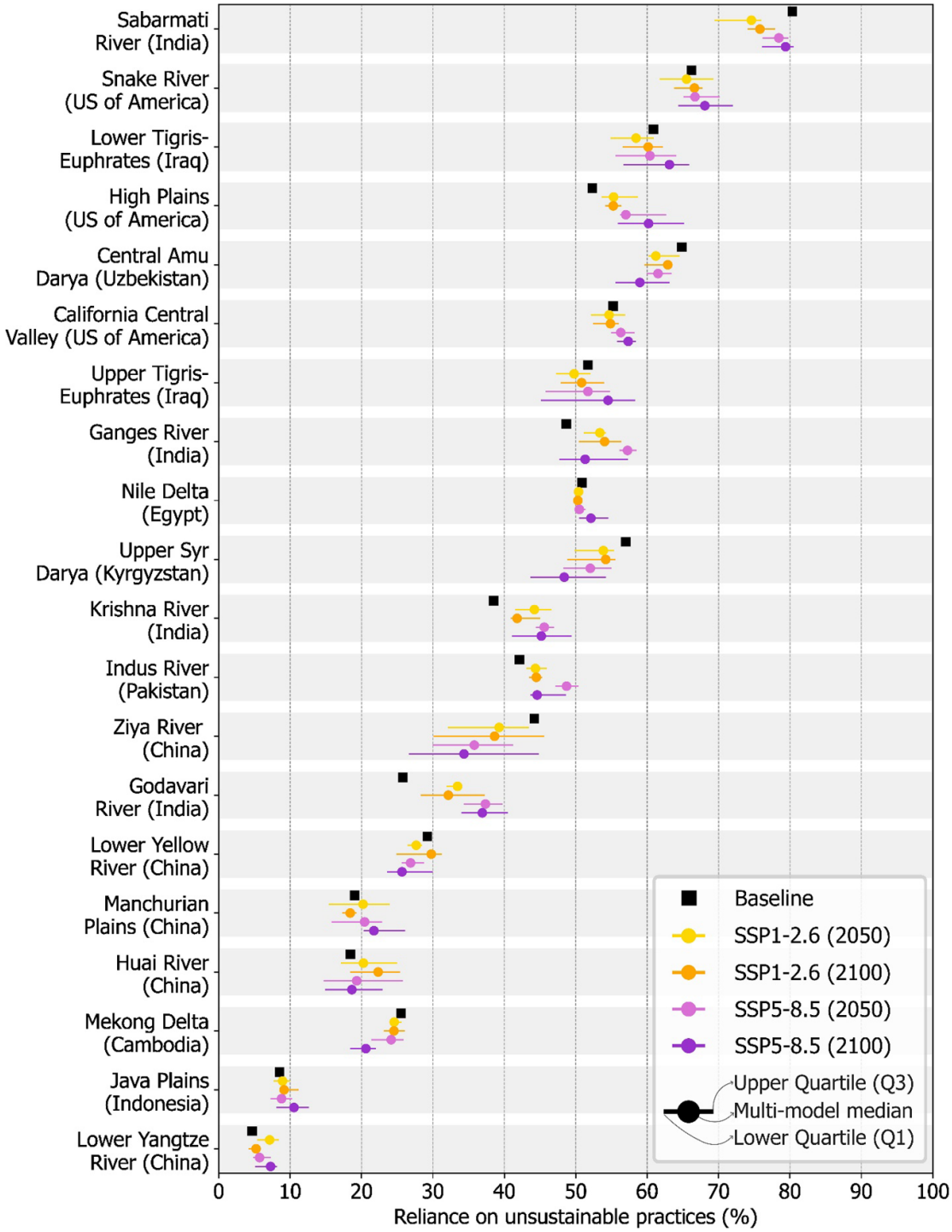

Figure 5. Multi-model median ensemble percentages of reliance on unsustainable practices under baseline conditions and relative changes under SSP1-2.6 and SSP5-8.5 scenarios for the top 20 irrigation regions by water consumption. Changes in baseline UIWC to total water consumption (%) under SSP1-2.6 in 2050 and 2100, and under SSP1-8.5 in 2050 and 2100. The data points display the median values for each scenario with horizontal lines indicating the interquartile range as result of the multi-model ensemble of 10 combinations between two hydrological models (H08 and WaterGAP2-2e) and five climate models (IPSL-CM6A-LR, UKESM1-0-LL, GFDL ESM4, MPI-ESM1.2-HR, and MRI-ESM2.0).

Under the SSP1-2.6 scenario, the Mediterranean basin, the Indian Peninsula, and western Australia are projected to see the largest increase in reliance on UIWC, with peaks up to +58% (Condado de Huelva) and +18% (Wide Bay-Burnett and Mahi River) by the end of the century, respectively (figure 5, supplementary figures 5(b) and (c)). While the west coast of North America will show improvements, the US Atlantic coast is expected to worsen, and the US High Plains will experience a 3% increase in reliance on UIWC (figure 5, supplementary figures 5(b) and (c)). By 2100, under the SSP1-2.6 scenario, substantial decreases in reliance on UIWC are projected in Saudi Arabia, ranging from −10% to −15%

across the 10 model combinations, particularly in the Al-Hasa Oasis, Al-Kharj Plains, and Inner Mongolia (figure 5, supplementary figures 5(b) and (c)).

In the SSP5-8.5 scenario, a global increase in reliance on unsustainable irrigation is expected, with exceptions in regions such as northeast China, Central Asia, and the Mississippi Delta, which may experience reductions (figure 5, supplementary figures 5(d) and (e)). Key hotspots for increased reliance will be the Indian Peninsula, southwestern Europe, Australia, and the North American plains (figures 4(d) and (e)). The Mediterranean basin is projected to see the most marked increases, with the coastal plains and main islands experiencing rises of +23% to +77%. Conversely, Central Africa, Central Asia, and parts of China may see decreases of up to −21% (figure 5, supplementary figures 5(d) and (e)).

In response to potential limitations regarding the interpretation of UIWC relative to total water consumption, we further analyzed the proportion of irrigation water use relative to total water consumption for each IR (supplementary figure 6). This additional metric helps disentangle regional reliance on irrigation from the broader context of total water use, addressing the influence of agricultural sector dominance on the original ratio. We calculated projected shifts in the proportion of irrigation water use (assuming other sectoral water uses remain constant at baseline levels) under both low- (SSP1-2.6) and high-emissions (SSP5-8.5) scenarios for mid- (2050) and late-century (2100) periods. Under baseline conditions (2001–2010), many IRs (e.g. Sabarmati, Krishna, Central Amu Darya, and Indus River basins) already exhibit extremely high irrigation shares (>95%), underscoring their critical dependence on irrigation to sustain agricultural productivity. Future projections suggest that such dependence remains persistently high across most IRs, with limited variation (<5%) under SSP1-2.6, but larger changes (up to +11%) under SSP5-8.5, particularly in northeast China (e.g. Manchurian Plains, Lower Yangtze, Huai River). These findings highlight that, regardless of the emissions pathway, the global food production system remains structurally dependent on unsustainable irrigation practices.

4. Discussion

This study projects the volume of future unsustainable irrigation water consumption and the reliance on unsustainable irrigation practices under climate change scenarios, quantifying when and where pronounced changes will occur in the world's irrigated regions. The findings indicate an exacerbation in UIWC, particularly under the high-emission SSP5-8.5 scenario, where a rapid decline in water sustainability is expected by mid-century. Conversely, the SSP1-2.6 scenario offers a more optimistic outlook, with some regions potentially maintaining water sustainability through the end of the century. These results underscore the importance of mitigating climate change to ensure sustainable irrigation practices. The two climate change scenarios show distinct trends in UIWC, with marked changes across decades. The range of outcomes is wider under the high-emission SSP5-8.5 scenario compared to the more sustainable SSP1-2.6 scenario, reflecting greater uncertainty with higher emissions. The spread in projected UIWC resulting from different combinations of climate and hydrological models is comparable in magnitude to the differences observed between emission scenarios (figure 3). This finding underscores those uncertainties arising from model structure (including the representation of climatic drivers, hydrological processes, and their coupled interactions) can influence future projections as strongly as the assumed socio-economic pathways. The comparable weight of scenario-driven and model-driven uncertainty highlights the critical importance of using multi-model ensemble frameworks. Relying on a single climate-hydrological model could therefore lead to substantial under- or overestimation of future irrigation water demands, with significant implications for adaptation planning and water resource management under climate change. Notably, the ensemble spread arising from structural differences across climate and hydrological models is comparable to the gap between the two emissions pathways. This comparability confirms that model uncertainty can be as influential as socio-economic uncertainty and underscores the need for ensemble-based risk assessments. The variability in the results presented in this study further reinforces the complexity of predicting the possible conditions to be faced in the coming decades. A clearer picture of future trajectories allows to better inform, manage, and invest in strategic adaptation measures against climate-induced water scarcity.

Although the dominant global signal is an increase in UIWC, our simulations also reveal regions where the share of unsustainable irrigation declines (figure 2), due to modelled gains in renewable blue water availability, slower irrigation growth, or improvements in conveyance efficiency. A clear example is the Sabarmati River, where UIWC increases in all scenarios (figure 3(a)), yet the ratio of UIWC to total water withdrawals declines (figure 5). This occurs because non-agricultural consumptions are held constant, so total water consumption grows almost entirely with irrigation. When part of this additional irrigation demand is met by increases in renewable water supply, the unsustainable fraction grows more slowly than the total, leading to a lower ratio. Supplementary figure 6 confirms that irrigation already represents ∼98%–99% of total water consumptions in the Sabarmati, a dominance maintained in future projections. The specific magnitude of change, however, remains uncertain due to the

high inter-model spread in precipitation and blue water projections for north-western India [58, 59]. This case highlights the heterogeneous nature of climate impacts on irrigation sustainability. Even when trends are not statistically significant (supplementary table 1), directional changes that persist or appear consistently across models may still provide early indications of evolving irrigation stress. Regular reassessment of these trajectories is essential, as natural variability and limited time series can obscure emerging trends, and overlooking such signals may delay timely adaptation responses [60, 61].

While half of global irrigation water use has historically relied on unsustainable practices [10], increasing pressure on groundwater resources will likely push IRs to adopt more sustainable water management strategies [62]. This change is becoming increasingly necessary as the physical and economic limits of groundwater depletion become more evident [63]. Surface water reservoirs may offer a temporary buffer against water scarcity [64],but the capacity to stabilize freshwater supplies is limited by changing climate conditions [65]. The current framework of the global food trade also plays a key role in these water imbalances across geographical areas and disconnection between consumers and the water resources they rely on [10, 15, 66]. Major exporters such as India, Pakistan, Mexico, Spain, and the United States will need to limit support for importers (China, Bangladesh, the European Union, and the United States itself), trying not to exacerbate internal pressure on water resources further [10, 15]. Although trade roles can vary over time and by commodity, these countries have been identified as key actors in the global exchange of food products with high embedded virtual water content. Importing countries, in turn, should push for and foster international cooperation to monitor and regulate unsustainable virtual water flows by requiring certifications attesting to sustainable irrigation practices for imported products [10, 15]. In parallel, expressing UIWC on a per-unit-area basis (mm yr^{-1}) helps expose concentrated pressure points that may remain hidden when only absolute volumes are considered, thereby guiding more spatially targeted adaptation measures (figure 3(b)). The increases in UIWC detected in most IRs lead surface and groundwater resources to reach a point where their extraction exceeds replenishment, resulting in irreversible ecological damage and water depletion [67]. This phenomenon is particularly critical as many areas already rely heavily on non-renewable groundwater to support agricultural production [15, 68]. Our water balance integrates both surface water and groundwater availability; however, it does not capture the spatial heterogeneity of groundwater recharge or distinguishes between shallow and deep aquifer use. Rather than introducing uncertain assumptions, our method prioritizes internal consistency and ensemble robustness. By flagging regions where irrigation exceeds renewable supply, our estimates help identify areas most likely to rely on non-renewable sources, whether through surface storage depletion or unsustainable groundwater consumption. This supports the prioritization of conjunctive use of surface and groundwater, as well as aquifer monitoring, at the regional scale [69, 70]. Our study is part of a growing body of research examining the global water crisis [71]. The Nile Delta and the California Central Valley present a particularly concerning situation. Although our projections indicate stability or relative improvement in UIWC, the ability to maintain sustainable irrigation practices in these regions is largely compromised with the current UIWC of about 18.2 km^3 yr^{-1} and 9.3 km^3 yr^{-1} in the Nile Delta and in the California Central Valley, respectively (figure 3(a)). On the other hand, there is still leeway in some regions, such as the Po Valley, which, despite ranking among the most affected regions by 2100, has relatively low baseline UIWC (0.2 km^3 yr^{-1}) and reliance (below 5%) on UIWC (figure 4(a), supplementary figure 5(a)). Integrated water resources management that includes investments in resilient infrastructure to improve innovative water storage, wastewater re-use, water transfer, and desalination solutions [38, 72–78] would bring concrete improvements. Furthermore, IRs shared by multiple countries present unique challenges for sustainable water management due to their transboundary nature, complicating governance and resource allocation [79, 80]. Projected UIWC trends for the Hispaniola Island, the Mekong Delta, the Douro River basin, Cyprus, and the Eastern Mediterranean Coast demonstrate how water scarcity can further stress the current transboundary problems linked to the water competition for agriculture, food security, and geopolitical stability [81]. While cumulative accounting of UIWC could be informative for certain long-term budgeting analyses [41], we intentionally focused on decade-by-decade trajectories because they align more closely with planning horizons for infrastructure investment, policy cycles, and adaptive water governance. Moreover, such a global view can serve as a blueprint for prioritizing regional scale studies, helping to identify regions where risks start to emerge. By presenting results using multi-model simulations in the 21st century, our study provides quantitative and time-based pivotal information for each IR.

Data availability statement

The data that support the findings of this study are openly available at the following URL/DOI: 10.5281/zenodo.13967727.

Conflict of interest

The authors declare no conflict of interest.

Author contributions

L R conceived the study; All authors designed research; A C, M S performed research; A C analyzed data; A C and L R wrote the study with input from M S.

ORCID iDs

Andrea Citrini 0000-0002-1352-2356
Matteo Sangiorgio 0000-0003-1624-6809
Lorenzo Rosa 0000-0002-1280-9945

References

[1] Rosa L 2022 Adapting agriculture to climate change via sustainable irrigation: biophysical potentials and feedbacks *Environ. Res. Lett.* **17** 063008
[2] Rezaei E E, Webber H, Asseng S, Boote K, Durand J L, Ewert F, Martre P and MacCarthy D S 2023 Climate change impacts on crop yields *Nat. Rev. Earth Environ.* **4** 831–46
[3] McDermid S *et al* 2023 Irrigation in the Earth system *Nat. Rev. Earth Environ.* **4** 435–53
[4] Qin Y, Mueller N D, Siebert S, Jackson R B, AghaKouchak A, Zimmerman J B, Tong D, Hong C and Davis S J 2019 Flexibility and intensity of global water use *Nat. Sustain.* **2** 515–23
[5] Beltran-Peña A, Rosa L and D'Odorico P 2020 Global food self-sufficiency in the 21st century under sustainable intensification of agriculture *Environ. Res. Lett.* **15** 095004
[6] Wang X *et al* 2021 Global irrigation contribution to wheat and maize yield *Nat. Commun.* **12** 1235
[7] Droppers B, Supit I, Van Vliet M T and Ludwig F 2021 Worldwide water constraints on attainable irrigated production for major crops *Environ. Res. Lett.* **16** 055016
[8] Qin Y, Abatzoglou J T, Siebert S, Huning L S, AghaKouchak A, Mankin J S, Hong C, Tong D, Davis S J and Mueller N D 2020 Agricultural risks from changing snowmelt *Nat. Clim. Change* **10** 459–65
[9] Beltran-Peña A A, Rhoades A, Burakowski E, Girotto M, Michalak A M, Diffenbaugh N S, Inda-Diaz H and D'Odorico P 2025 Future implications of enhanced hydroclimate variability and reduced snowpack on California's water resources *Environ. Res. Water* **1** 025004
[10] Rosa L, Chiarelli D D, Tu C, Rulli M C and D'Odorico P 2019 Global unsustainable virtual water flows in agricultural trade *Environ. Res. Lett.* **14** 114001
[11] Brauman K A, Richter B D, Postel S, Malsy M and Flörke M 2016 Water depletion: an improved metric for incorporating seasonal and dry-year water scarcity into water risk assessments *Elementa* **4** 000083
[12] Jägermeyr J, Pastor A, Biemans H and Gerten D 2017 Reconciling irrigated food production with environmental flows for sustainable development goals implementation *Nat. Commun.* **8** 15900
[13] Scanlon B R, Rateb A, Pool D R, Sanford W, Save H, Sun A, Long D and Fuchs B 2021 Effects of climate and irrigation on GRACE-based estimates of water storage changes in major US aquifers *Environ. Res. Lett.* **16** 094009
[14] Tuninetti M, Tamea S and Dalin C 2019 Water debt indicator reveals where agricultural water use exceeds sustainable levels *Water Resour. Res.* **55** 2464–77
[15] Dalin C, Wada Y, Kastner T and Puma M J 2017 Groundwater depletion embedded in international food trade *Nature* **543** 700–4
[16] Mekonnen M M and Hoekstra A Y 2020 Blue water footprint linked to national consumption and international trade is unsustainable *Nat. Food* **1** 792–800
[17] Jones E R, Bierkens M F P and Van Vliet M T H 2024 Current and future global water scarcity intensifies when accounting for surface water quality *Nat. Clim. Change* **14** 629–35
[18] Van Vliet M T H *et al* 2023 Global river water quality under climate change and hydroclimatic extremes *Nat. Rev. Earth Environ.* **4** 687–702
[19] Wang M *et al* 2024 A triple increase in global river basins with water scarcity due to future pollution *Nat. Commun.* **15** 880
[20] Rosa L, Chiarelli D D, Rulli M C, Dell'Angelo J and D'Odorico P 2020 Global agricultural economic water scarcity *Sci. Adv.* **6** eaaz6031
[21] Rosa L, Rulli M C, Davis K F, Chiarelli D D, Passera C and D'Odorico P 2018 Closing the yield gap while ensuring water sustainability *Environ. Res. Lett.* **13** 104002
[22] IPCC 2023 Climate change 2023: synthesis report Contribution of Working Groups I, II and III to the Sixth Assessment Report of the Intergovernmental Panel on Climate Change ed H Lee and J Romero (Core Writing Team) ed pp 35–115
[23] Konapala G, Mishra A K, Wada Y and Mann M E 2020 Climate change will affect global water availability through compounding changes in seasonal precipitation and evaporation *Nat. Commun.* **11** 3044
[24] Lesk C, Anderson W, Rigden A, Coast O, Jägermeyr J, McDermid S, Davis K F and Konar M 2022 Compound heat and moisture extreme impacts on global crop yields under climate change *Nat. Rev. Earth Environ.* **3** 872–89
[25] Singh B K, Delgado-Baquerizo M, Egidi E, Guirado E, Leach J E, Liu H and Trivedi P 2023 Climate change impacts on plant pathogens, food security and paths forward *Nat. Rev. Microbiol.* **21** 640–56
[26] Scanlon B R *et al* 2023 Global water resources and the role of groundwater in a resilient water future *Nat. Rev. Earth Environ.* **4** 87–101
[27] Deng Q *et al* 2025 Deepening water scarcity in breadbasket nations *Nat. Commun.* **16** 1110
[28] Trnka M *et al* 2019 Mitigation efforts will not fully alleviate the increase in water scarcity occurrence probability in wheat-producing areas *Sci. Adv.* **5** eaau2406
[29] Elliott J *et al* 2014 Constraints and potentials of future irrigation water availability on agricultural production under climate change *Proc. Natl Acad. Sci.* **111** 3239–44
[30] Fitton N *et al* 2019 The vulnerabilities of agricultural land and food production to future water scarcity *Glob. Environ. Change* **58** 101944
[31] Huang Z, Liu X, Sun S, Tang Y, Yuan X and Tang Q 2021 Global assessment of future sectoral water scarcity under adaptive inner-basin water allocation measures *Sci. Total Environ.* **783** 146973
[32] Liu X, Liu W, Tang Q, Liu B, Wada Y and Yang H 2022 Global agricultural water scarcity assessment incorporating blue and green water availability under future climate change *Earths Future* **10** e2021EF002567
[33] Liu X, Liu W, Liu L, Tang Q, Liu J and Yang H 2021 Environmental flow requirements largely reshape global surface water scarcity assessment *Environ. Res. Lett.* **16** 104029
[34] Schewe J *et al* 2014 Multimodel assessment of water scarcity under climate change *Proc. Natl Acad. Sci.* **111** 3245–50
[35] Zhao F *et al* 2017 The critical role of the routing scheme in simulating peak river discharge in global hydrological models *Environ. Res. Lett.* **12** 075003
[36] Mehta P, Siebert S, Kummu M, Deng Q, Ali T, Marston L, Xie W and Davis K F 2024 Half of twenty-first century global irrigation expansion has been in water-stressed regions *Nat. Water* **2** 254–61

[37] O'Neill B C et al 2016 The Scenario Model Intercomparison Project (Scenariomip) for CMIP6 Geosci. Model Dev. 9 3461–82
[38] Kahn M, Sangiorgio M and Rosa L 2025 Potential of wastewater reuse to alleviate water scarcity under future warming scenarios Environ. Res. Lett. 20 034012
[39] Rosa L, Ragettli S, Sinha R, Zhovtonog O, Yu W and Karimi P 2024 Regional irrigation expansion can support climate-resilient crop production in post-invasion Ukraine Nat. Food 5 684–92
[40] Rosa L, Chiarelli D D, Sangiorgio M, Beltran-Peña A A, Rulli M C, D'Odorico P and Fung I 2020 Potential for sustainable irrigation expansion in a 3 °C warmer climate Proc. Natl Acad. Sci. 117 29526–34
[41] Rosa L and Sangiorgio M 2025 Global water gaps under future warming levels Nat. Commun. 16 1192
[42] Meinshausen M et al 2020 The shared socio-economic pathway (SSP) greenhouse gas concentrations and their extensions to 2500 Geosci. Model Dev. 13 3571–605
[43] Lehner B and Grill G 2013 Global river hydrography and network routing: baseline data and new approaches to study the world's large river systems Hydrol. Process. 27 2171–86
[44] Geological Survey (US) 1977 National Handbook of Recommended Methods for Water-Data Acquisition vol 1 (U.S. Government Printing Office)
[45] Rosa L and He L 2025 Global multi-model projections of green water scarcity risks in rainfed agriculture under 1.5 °C and 3 °C warming Agric. Water Manag. 314 109519
[46] Mekonnen M M and Hoekstra A Y 2016 Four billion people facing severe water scarcity Sci. Adv. 2 e1500323
[47] Sutanudjaja E H et al 2018 PCR-GLOBWB 2: a 5 arcmin global hydrological and water resources model Geosci. Model Dev. 11 2429–53
[48] Hanasaki N, Yoshikawa S, Pokhrel Y and Kanae S 2018 A global hydrological simulation to specify the sources of water used by humans Hydrol. Earth Syst. Sci. 22 789–817
[49] Yoshida T, Hanasaki N, Nishina K, Boulange J, Okada M and Troch P A 2022 Inference of parameters for a global hydrological model: identifiability and predictive uncertainties of climate-based parameters Water Resour. Res. 58 e2021WR030660
[50] Müller Schmied H et al 2023 The global water resources and use model WaterGAP v2.2e: description and evaluation of modifications and new features (available at: https://doi.org/10.5194/gmd-2023-213)
[51] Gosling S N et al 2024 ISIMIP3a simulation data from the global water sector ISIMIP Repository (available at: 10.48364/ISIMIP.398165.2)
[52] He L and Rosa L 2023 Solutions to agricultural green water scarcity under climate change PNAS Nexus 2 pgad117
[53] Pendergrass A G, Knutti R, Lehner F, Deser C and Sanderson B M 2017 Precipitation variability increases in a warmer climate Sci. Rep. 7 17966
[54] Huang Z et al 2018 Reconstruction of global gridded monthly sectoral water withdrawals for 1971–2010 and analysis of their spatiotemporal patterns Hydrol. Earth Syst. Sci. 22 2117–33
[55] Zhang X, Zhang Y, Tian J, Ma N and Wang Y-P 2022 CO_2 fertilization is spatially distinct from stomatal conductance reduction in controlling ecosystem water-use efficiency increase Environ. Res. Lett. 17 054048
[56] De Graaf I E M, Gleeson T, (Rens) Van Beek L P H, Sutanudjaja E H and Bierkens M F P 2019 Environmental flow limits to global groundwater pumping Nature 574 90–94
[57] Pastor A V, Ludwig F, Biemans H, Hoff H and Kabat P 2014 Accounting for environmental flow requirements in global water assessments Hydrol. Earth Syst. Sci. 18 5041–59
[58] Hasson S U, Pascale S, Lucarini V and Böhner J 2016 Seasonal cycle of precipitation over major river basins in South and Southeast Asia: a review of the CMIP5 climate models data for present climate and future climate projections Atmos. Res. 180 42–63
[59] Katzenberger A, Schewe J, Pongratz J and Levermann A 2021 Robust increase of Indian monsoon rainfall and its variability under future warming in CMIP6 models Earth Syst. Dyn. 12 367–86
[60] Weatherhead E C, Stevermer A J and Schwartz B E 2002 Detecting environmental changes and trends Phys. Chem. Earth ABC 27 399–403
[61] Tjiputra J F, Negrel J and Olsen A 2023 Early detection of anthropogenic climate change signals in the ocean interior Sci. Rep. 13 3006
[62] Greve P et al 2018 Global assessment of water challenges under uncertainty in water scarcity projections Nat. Sustain. 1 486–94
[63] Turner S W D, Hejazi M, Yonkofski C, Kim S H and Kyle P 2019 Influence of groundwater extraction costs and resource depletion limits on simulated global nonrenewable water withdrawals over the twenty-first century Earths Future 7 123–35
[64] Schmitt R J P, Rosa L and Daily G C 2022 Global expansion of sustainable irrigation limited by water storage Proc. Natl Acad. Sci. 119 e2214291119
[65] Liu L, Parkinson S, Gidden M, Byers E, Satoh Y, Riahi K and Forman B 2018 Quantifying the potential for reservoirs to secure future surface water yields in the world's largest river basins Environ. Res. Lett. 13 044026
[66] Mekonnen M M et al 2024 Trends and environmental impacts of virtual water trade Nat. Rev. Earth Environ. 5 890–905
[67] Gleick P H and Palaniappan M 2010 Peak water limits to freshwater withdrawal and use Proc. Natl Acad. Sci. 107 11155–62
[68] Niazi H, Wild T B, Turner S W D, Graham N T, Hejazi M, Msangi S, Kim S, Lamontagne J R and Zhao M 2024 Global peak water limit of future groundwater withdrawals Nat. Sustain. 7 413–22
[69] Scanlon B R, Reedy R C, Faunt C C, Pool D and Uhlman K 2016 Enhancing drought resilience with conjunctive use and managed aquifer recharge in California and Arizona Environ. Res. Lett. 11 035013
[70] Sekar A, Valliammai A, Nagarajan M, Sivakumar S D, Baskar M and Sujitha E 2024 Conjunctive use in water resource management: current trends and future directions Water Supply 24 3881–904
[71] Liu J et al 2024 Timing the first emergence and disappearance of global water scarcity Nat. Commun. 15 7129
[72] Khondoker M, Mandal S, Gurav R and Hwang S 2023 Freshwater shortage, salinity increase, and global food production: a need for sustainable irrigation water desalination—a scoping review Earth 4 223–40
[73] Schmitt R J P and Rosa L 2024 Dams for hydropower and irrigation: trends, challenges, and alternatives Renew. Sustain. Energy Rev. 199 114439
[74] Shumilova O, Tockner K, Thieme M, Koska A and Zarfl C 2018 Global water transfer megaprojects: a potential solution for the water-food-energy nexus? Front. Environ. Sci. 6 150
[75] Siddik A B Md, Dickson K E, Rising J, Ruddell B L and Marston L T 2023 Interbasin water transfers in the United States and Canada Sci. Data 10 27
[76] Sun S, Tang Q, Konar M, Fang C, Liu H, Liu X and Fu G 2023 Water transfer infrastructure buffers water scarcity risks to supply chains Water Res. 229 119442
[77] Van Vliet M T H, Jones E R, Flörke M, Franssen W H P, Hanasaki N, Wada Y and Yearsley J R 2021 Global water scarcity including surface water quality and expansions of clean water technologies Environ. Res. Lett. 16 024020

[78] Zhang Y and Shen Y 2019 Wastewater irrigation: past, present, and future *WIREs Water* **6** e1234
[79] Hussein H, Menga F and Greco F 2018 Monitoring transboundary water cooperation in SDG 6.5.2: how a critical hydropolitics approach can spot inequitable outcomes *Sustainability* **10** 3640
[80] Mianabadi A, Davary K, Mianabadi H and Karimi P 2020 International environmental conflict management in transboundary river basins *Water Resour. Manag.* **34** 3445–64
[81] Gökçekuş H and Bolouri F 2023 Transboundary waters and their status in today's water-scarce world *Sustainability* **15** 4234